4th International Conference on Silicon Photovoltaics, SiliconPV 2014

Multi-wire interconnection of busbar-free solar cells

Johann Walter[a],*, Marco Tranitz[a], Michael Volk[b], Christian Ebert[b], Ulrich Eitner[a]

[a]Fraunhofer ISE, Heidenhofstraße 2, Freiburg 79110, Germany
[b]SCHMID Group | Gebr. SCHMID GmbH, Robert-Bosch-Str. 32-36, Freudenstadt 72250, Germany

Abstract

The interconnection of busbar-free solar cells by multiple wires is a simple and evolutionary concept to lower the cost of PV modules by reducing silver consumption for the front side metallization and to increase the module efficiency by lower series resistance and improved light harvesting. A 0.33 % absolute higher performance of MBB against the established H-pattern solar cell has already been demonstrated by Braun [1]. This work focuses on the interconnection of Multi Busbar cells (MBB) by infrared soldering and the optimization of the front metallization design in order to achieve reliable solder joints. We find the following factors to be crucial for the MBB-interconnection process: a homogeneous radiation field, a process-adapted down-holder device, a homogeneous wire coating, a precise wire positioning and a method to absorb the wire expansion caused by the elevated solder temperatures. We measure peel forces up to 5.7 N/mm as the average peel force value of five pad rows from the center of two MBB cells containing 160 soldered pads. Furthermore a one-cell MBB-module shows a more homogeneous series resistance with an approximately 0.3 Ωcm^2 lower series resistance compared to a one-cell 3-busbar module, which we determine by C-DCR (coupled determination of the dark saturation current and the series resistance). Finally two 20-cell MBB modules manufactured with an automated MBB-stringer pass the TC-200 test without significant changes in IV, EL and module optical appearance.

Keywords: solar cell; multi busbar; interconnection; PV module; wire interconnection

* Corresponding author. Tel.: +49-761-4588-5824; fax: +49-761-4588-9193
   E-mail address: johann.walter@ise.fraunhofer.de

1. Introduction

In order to reduce the amount of silver for the metallization of crystalline silicon solar cells and to improve the module efficiency the current trend in interconnection technology is to move from three busbars to four or five busbars [2]. Continuing the idea of increasing the number of busbars and reducing the finger cross sections results in the interconnection of busbar free solar cells.

Meyer Burger's SmartWire Connection Technology (SWCT) concept [3] is based on the Day4Energy technology [4] which was commercialized between 2007 and 2011. It favours 38 wires and interconnects during the lamination process at 160 °C using a low melting-temperature alloy. The main idea of SCHMID's Multi Busbar concept (MBB) is to solder the wires onto the cells before lamination. This concept currently favors 15 solder coated copper wires and uses infrared soldering.

The benefit of wire interconnection compared to the three-busbar (3BB) design has been published by Braun confirming an efficiency gain of 0.33 % absolute and a lower silver consumption of 50 % [1, 5-7]. Braun attributes the efficiency gain to improved module optics, due to the round shaped wires, and the shorter current paths in the finger metallization. Schindler investigates the influence of the copper wire diameter of 250 µm and 300 µm on the peel force, observing no considerable differences in terms of peel force and fracture mode [8]. However, increasing the wire diameter enables a lower series resistance along with higher shadowing of the active cell area.

2. Interconnection of multi busbar cells

2.1. Soldering tests

We perform preliminary soldering tests on Gen 2 cells in order to compare infrared, contact, hot air, laser and induction soldering. Due to the larger pads on the cell, higher adhesive forces can be observed at the beginning and the end of the curve. In figure 1 representative peel results of the inner pads are shown, to compare the different soldering methods. Soldering by infrared, contact soldering and hot air results in a higher number of connected solder pads, compared to soldering by laser or induction.
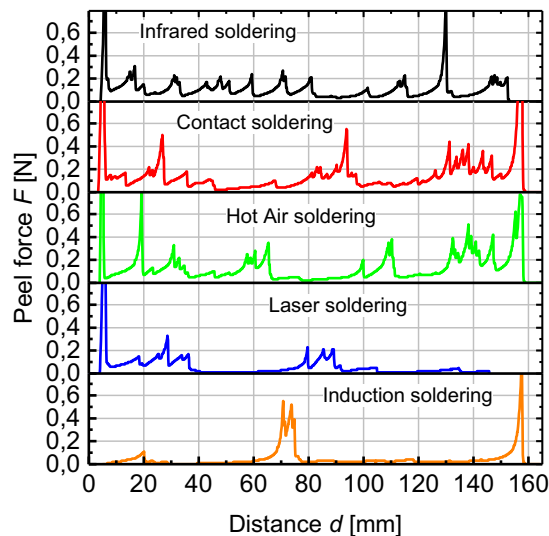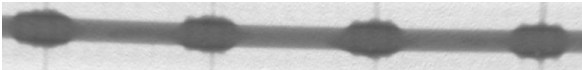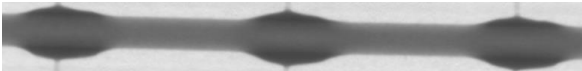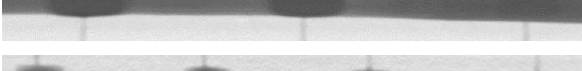

Fig. 1. Adhesive force measurements of different soldering methods.

We analyse the solder joints with X-Ray to investigate the solder distribution on the pad and to inspect the joints for either voids or any non-uniformity. Table 1 shows the X-Ray images of the different solder methods. We found no

major voids. Hot air soldering shows the most inhomogeneous solder distribution on the pad. This is probably due to the air stream pressure in the equipment we use for preliminary testing.

Table 1. X-Ray images of different solder techniques.

Solder technique	X-Ray image
Infrared	
Contact soldering	
Hot air	
Laser	
Induction	

We come to the conclusion that infrared soldering meets our requirements to interconnect MBB cells in terms of soldering process speed, generating reproducible and stable solder joints with a high adaptability for different down holder designs. We find out that a very homogeneous radiation field is critical to achieve a uniform temperature distribution over the entire cell. This means the shadow and the reflection caused by the down-holder must be considered. A cross section of a pad soldered by infrared is shown figure 2. We assume the large wetting angle is due to the small pad width.
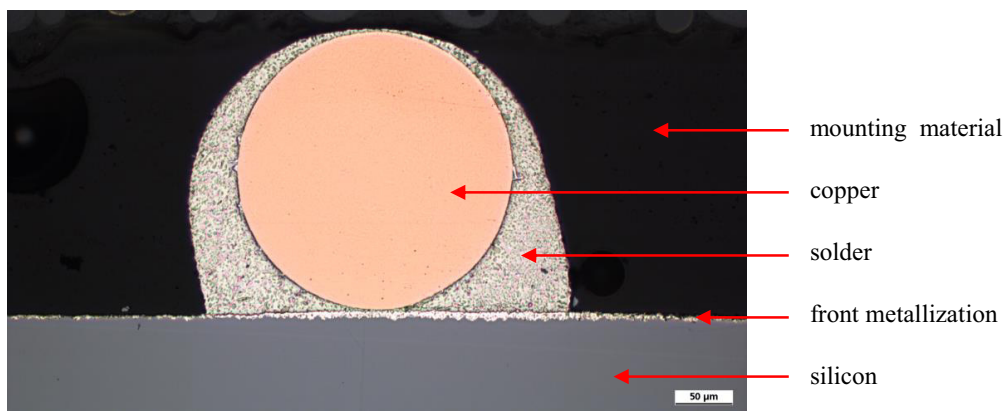

Fig. 2. Cross section of the wire soldered to a solder pad.

2.2. Wire

Beyond a stable solder process the properties of the used solder wire are crucial. From soldering experiments we determine that an inhomogeneous solder coating on the wire may lead to poor solder joints. Figure 4 demonstrates two metallographic cross-section images of two different wires.
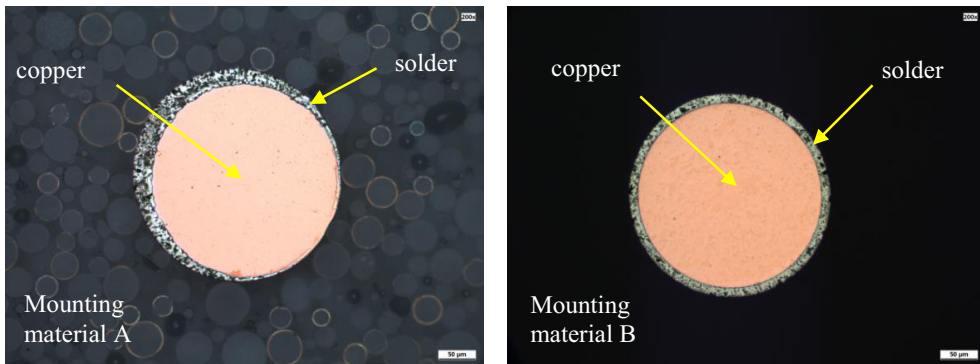
Fig. 3. Copper wire coated with solder (left: inhomogeneous; right: homogeneous). Mounting material has been changed for preparation reasons.

The optimal process parameters are crucial not only for stable solder joints but also to control the expansion of the wire which is due to the heating process as illustrated in figure 4a. A well designed down-holder can control the wire expansion and reduces the risk of wire displacement from the pad as demonstrated in figure 4b. Since the wire has a diameter of 270 µm or 330 µm and the center pad a width of 450 µm for the Gen 2 cell (Fig. 4), high positioning accuracy has to be fulfilled by the combined tabber stringer (CTS). If the wire is not centered on the pad (Fig. 4c), the risk of missing or failing joints increases. Wider pads as they are introduced in Gen 3 facilitate this handling issue.
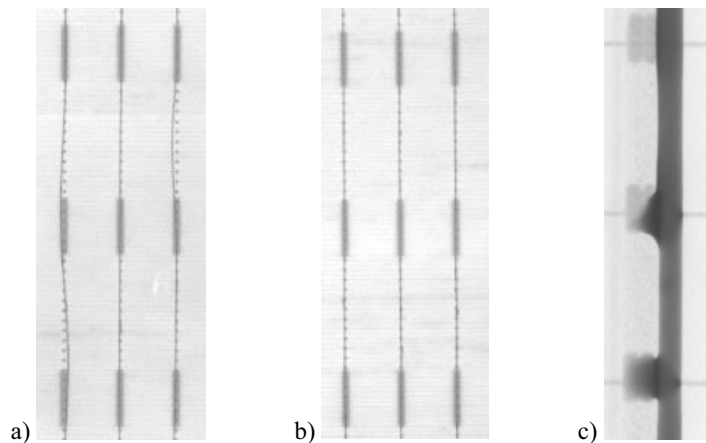

Fig. 4. a) Heavy wire expansion caused by a non-optimal heating process; b) Accurate wire positioning and optimal heating process; c) Wire positioning failure.

3. Variation of the front side metallization and adhesive force measurements

The adhesion force of three different MBB cell generations is presented (Fig 5). Generation 1 (Gen 1) have no solder pads on the front side and the wires have to be directly soldered to the fingers. The generation 2 (Gen 2) design contains 350 x 450 µm² solder pads on each finger at the soldering positions for the 15 wires. Additionally, there are extended pads (750 x 1800 µm²) located between the 4th and 5th finger to support the wire adhesion along the edge of the cell. In generation 3 (Gen 3) the smaller solder pads have an area of 1000 x 400 µm² and are located on every 6th finger connected via narrow silver paths. The Gen3-design supports the transport of the current to the

next pad of the pad row in case of an unconnected pad. Similar to Gen 2 it features wider pads (1000 x 1900 μm²) alongside the cell edge.
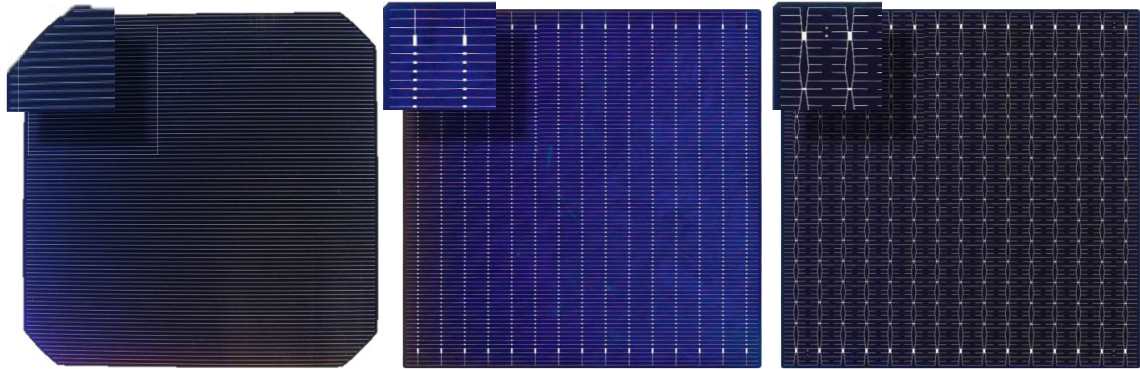

Fig. 5. Overview of MBB generations starting from the left: generation 1, generation 2, generation 3.

90° peel force measurements are carried out to assess the adhesion of the wires to the cells. Figure 6 shows such a peel force diagram exemplarily for Gen 3. We extract the maximum forces for every solder joint (in red) and generate boxplots as presented in figure 7. For the comparison of Gen 1, Gen 2 and Gen 3 we select the best peel force we measure from each generation. Above each boxplot the number of soldered pads is listed. However if few pads are not connected to the wire the influence in series resistance is negligible due to the large number of total solder joints.

Soldering on fingers has not proven successful. The forces achieved are far below the standard 1 N/mm threshold [9]. A soldered area width of 330 μm has been used as a reference to calculate the peel force per mm. Furthermore most of the fingers do not get connected to the wire. For this reason small pads are added in generation 2. Since we often find a wire detaching at the first soldered finger, on Gen 1 larger soldering pads are placed at the beginning and the end of a pad row. This improvement enables higher adhesion forces at the beginning or the end of a pad row (Fig. 1). The increased adhesive force from Gen 2 to Gen 3 is the result of changing the metallization printing method. Whereas silver plating is used for Gen 2, screen printing is applied to Gen 3. This result is also observed by Schindler [8]. To demonstrate the reproducibility of the peak forces, the middle five pads rows of two cells are analyzed and also displayed as box plots in figure 7.
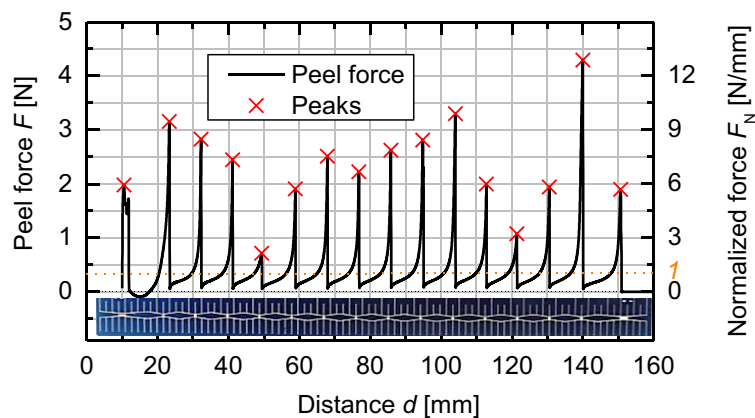

Fig. 6. Left: Adhesive force between wire and solder pads measured on a Zwick tensile testing machine modified for 90°-peel testing.
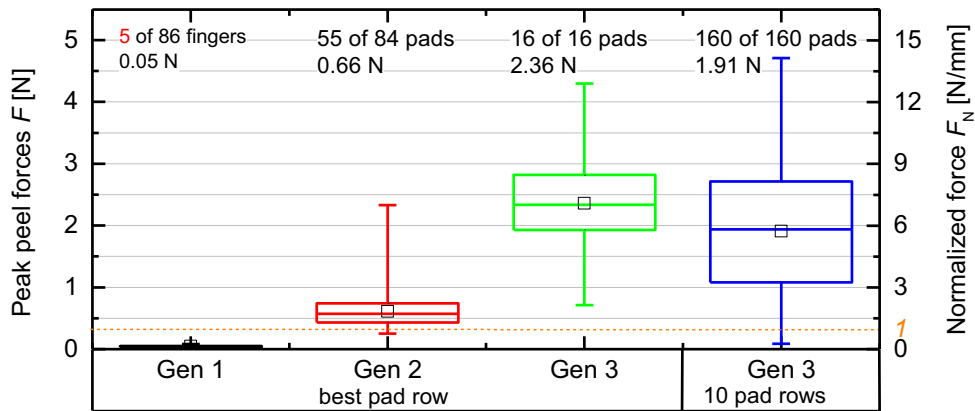
Fig. 7. Evolution of the best peel forces on the Multi Busbar technology presented for different cell generations.

4. Electrical properties

Six one-cell PV modules with Gen 2 cells are manufactured and measured by C-DCR [10]. A good agreement between the measured global series resistance from C-DCR and the series resistance determined by a flasher has been achieved. The difference might be due to the fact that the C-DCR voltage measurement is performed on module level and not on cell level.

Table 2. Series resistance determined from PL-R_S and IV-measurement.

	Global R_S from C-DCR [Ω*cm²]	Measured R_S from IV [Ω*cm²]
MBB	0,94	0,97
3BB	1,22	1,25

The MBB technology shows a more homogeneous and lower series resistance (Fig. 8) due to the increased number of current paths resulting in a more uniform current distribution. More wires lead to a shorter effective finger length and reduce series resistance loss in the fingers as shown in figure 8. Considering the significant impact of the finger resistance on the cell series resistance, this is a crucial advantage.
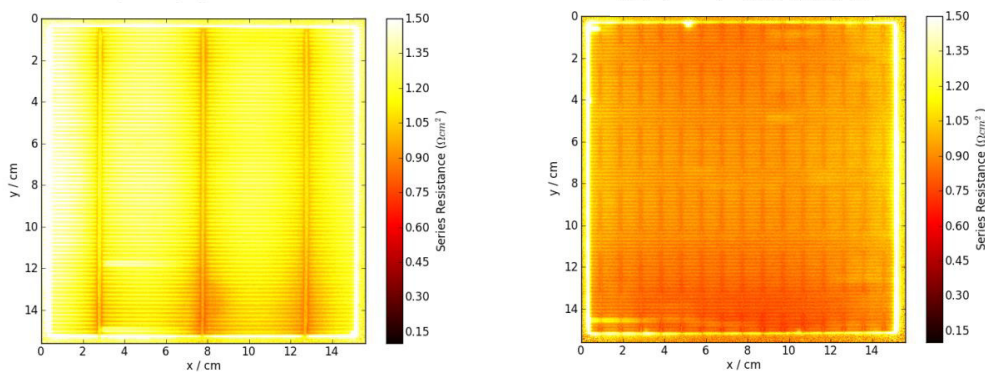

Fig. 8. Spatially resolved series resistance of one-cell modules determined by PL-Rs (left: 3BB, right: MBB).

The spatial resolved series resistance of the 3BB module ranges from 1.0 Ωcm² to 1.4 Ωcm² over large cell areas while for MBB the spatial resolved series resistance remains between 0.75 Ωcm² to 1.05 Ωcm² for MBB (Fig. 9). The minor average deviation of 0.146 Ωcm² (variance: 0.021 Ωcm²) for the MBB module emphasizes the more homogeneous series resistance distribution compared to the 3BB module, achieving an average deviation of 0.159 Ωcm² (variance: 0.025 Ωcm²).
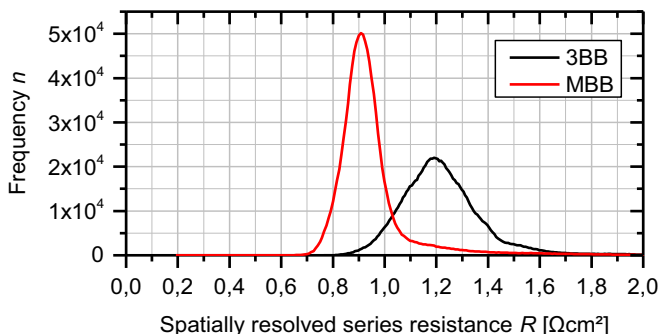

Fig. 9. Histogram distribution of the spatially resolved series resistance of the one-cell MBB and 3BB module of Fig. 8.

5. Reliability

To assess the thermo-mechanical stability of the interconnection method two 20-cell modules are manufactured by Schmid`s Multi Busbar Connector and are investigated by TC-200 at Fraunhofer ISE. The modules pass the test without considerable changes in the electrical parameters as shown in Tab. 3.

Table 3. IV-measurements before and after TC-200 performed by CalLab PV-Module at Fraunhofer ISE.

Mo-dule	I_{sc} [mA]		V_{oc} [V]		P_{mpp} [W]		I_{mpp} [A]		V_{mpp} [V]		FF [%]		η [%]	
M1	8.974	-0.2 %	12.556	+0.3 %	85.240	-0.2 %	8.433	-0.2 %	10.108	+0.0 %	75.64	-0.3 %	14.404	-0.2 %
	8.957		12.590		85.042		8.413		10.108		75.41		14.371	
M2	9.007	+0.1 %	12.573	+0.3 %	85.268	+0.0 %	8.438	+0.0 %	10.105	+0.0 %	75.30	-0.3 %	14.409	+0.0 %
	9.012		12.607		85.301		8.439		10.108		75.07		14.415	
Meas. Acc.	±1.9 %		±0.8 %		±2.2 %		±1.3 %		±2.5 %		±2.4 %		±2.7 %	

The EL images before and after TC-200 confirming the positive thermo-mechanical stability showing a good crack resistance. Exemplary the EL images of module M2 are presented in Fig 10.
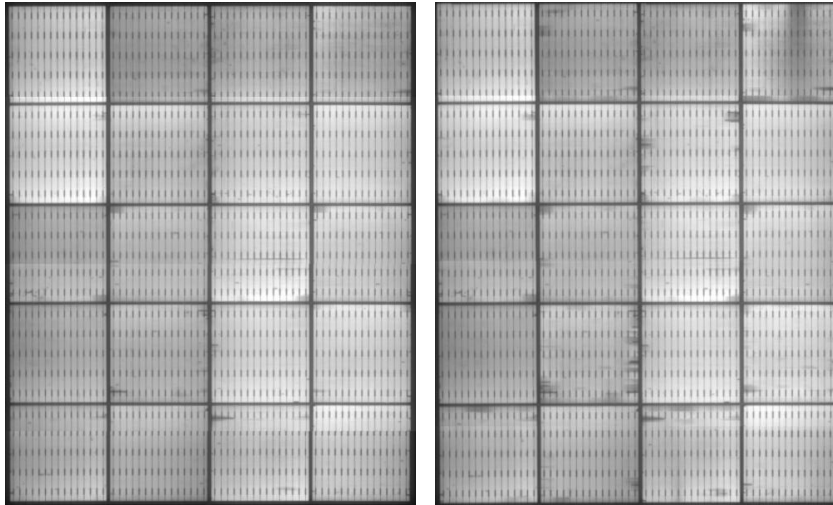
Fig. 10. EL images of M2 initial (left) and after TC-200 (right).

6. Conclusion

In this paper the results of preliminary soldering tests and the interconnection of Gen 1, Gen 2 and Gen 3 MBB solar cells are presented. Infrared soldering meets the requirements in terms of short process time for 84 x 15 solder pads (Gen 2), generating reproducible and stable solder joints. Gen 3 achieves maximum average peel forces of 5.7 N/mm, which is far beyond the standard 1 N/mm threshold. We analyze the five middle pad rows of two cells containing 160 pads, where we find all pads to be connected to the wire. Another factor influencing the soldering result is a homogenous solder coating around the Cu-wire since it may lead to insufficient solder joints.

The C-DCR measurement of one cell modules shows the spacially resolved series resistance for 3 busbar and Multi Busbar interconnection. It proves a more homogeneous series resistance distribution and lower series resistance of the Multi Busbar concept as a result of shorter effective current paths in the fingers. We observe more than 20 % series resistance reduction on one-cell module level.

20-cell MBB modules manufactured by the MBC passed the TC-200 test without any considerable change in IV characteristics and in EL images.

References

[1] S. Braun, G. Hahn, R. Nissler, Multi-Busbar solar cells and modules: high effiniencies and low silver consumption, in: Silicon PV, 2013.
[2] S.K. Chunduri, The buzz on busbars: Increasing the number of busbars - and the look of PV - is the latest trend in the CTS world, in: Photon International, pp. 84-105.
[3] T. Soederstroem, P. Papet, J. Ufheil, Smart wire connection technology, in: PVSEC, 2013.
[4] A. Schneider, L. Rubin, G. Rubin, Solar Cell Efficiency Improvement by New Metallization Techniques - the Day4 Electrode Concept, in: Photovoltaic Energy Conversion, Conference Record of the 2006 IEEE 4th World Conference on, 2006, pp. 1095-1098.
[5] S. Braun, G. Micard, G. Hahn, Solar cell improvement by using a multi busbar design as front electrode, Energy Procedia, 27 (2012) 227-233.
[6] S. Braun, G. Hahn, R. Nissler, C. Pönisch, D. Habermann, The Multi-Busbar design: an overview, in: 4th Metallization Workshop, 2013.

[7] S. Braun, R. Nissler, D. Habermann, G. Hahn, Highly efficient multi-busbar solar cells with Ag nano-particle front side metallization, in: EUPVSEC, 2013.

[8] S. Schindler, J. Schneider, C. Poenisch, R. Nissler, D. Habermann, Soldering process and material characterization of miniaturized contact structures of a newly developed multi busbar cell metallization concept, in: EUPVSEC, 2013.

[9] DIN EN 50461: Solar cells - Datasheet information and product data for crystalline silicon solar cells; German version EN 50461:2006.

[10] M. Glatthaar, J. Haunschild, M. Kasemann, J. Giesecke, W. Warta, S. Rein, Spatially resolved determination of dark saturation current and series resistance of silicon solar cells, in: phys. stat. sol. (RRL), 2010, pp. 13–15.